Advanced Studies in Biology, Vol. 4, 2012, no. 4, 175 - 194

Classification of Global Phase Portraits of Morris-Lecar Model for Spiking Neuron

B. Raesi

Department of Mathematics, Basic Sciences School, Shahed University, Tehran, Iran
P.O. Box: 18155/159, Zip 3319118651
raesi@shahed.ac.ir

M. Hassanpour-Ezatti

Department of Biology, Basic Sciences School, Shahed University,Tehran, Iran
P.O. Box: 18155/159, Zip 3319118651
hassanpm@yahoo.com

H. Zahmati

Department of Mathematics, Basic Sciences School, Shahed University, Tehran, Iran
P.O. Box: 18155/159, Zip 3319118651
zahmati460@gmail.com

Abstract

In this paper all possible global phase portraits of the Morris-Lecar Model with hyperbolic equilibrium points are classified. We use geometrical properties of nullclines and Poincaré-Bendixson theorem to omit impossible phase portraits. Finally some possible phase portraits for Morris-Lecar model are determined numerically.

Subject Classifications: 37E99, 92C20, 37N25, 92B05

Keywords: Phase portraite, Morris-Lecar model, Poincaré-Bendixson theorem

1 Introduction

This is the text of the introduction [1], [2]. The Morris-Lecar model (ML model) is one of the most famous spiking neuron models. It was introduced in 1981 by Morris and Lecar while they studied on Barnacle giant muscle fiber

[5]. Today's, this model is considered as a conductance based model of spiking neurons. Neurons which are able to generate spike or action potential are called spiking neurons. The first mathematical neuronal model (HH model) that describes action potential mechanism, was introduced by Hodgkin and Huxley in 1952 [1, 2, 3, 4]. It is also a conductance based model. Later Fitzhugh-Nagumo model [13, 14, 15, 10] and more general minimal conductance based models [7] were obtained as a simplified HH model (the dimension of differential equations in these models are reduced and parameter space is restricted). A simple neural model named single compartment minimal conductance based model is used by scientists for biophysical interpretation of excitable cell such as a neuron. To our best knowledge, a complete mathematical description of the structure of the phase portraits of ML model has not been given in the literature. In this paper in the case where ML model has three hyperbolic equilibrium points, all global phase portraits are classified with introducing three new concepts, Hopf point, segment and separator cycle. In some cases numerical examples are presented.

The structure of the paper is as follow: The fundamental concepts of conductance based models are introduced in section 2. Preliminary materials and some theorems that will be used in the rest of the paper are presented in section 3. In section 4, some necessary conditions for the existence of saddle-loops are determined. In section 5, in the case where three equilibrium points are hyperbolic, all possible global phase portraits are determined by using two new concepts which are named segment and separator cycle. In section 6, the results are generalized and it is shown that they are valid for $I_{Na,p} + I_K$ model (for more details about this model see [7]).

2 Conductance based model.

A class of mathematical models for spiking neuron, known as conductance-based ones, has their origins in the classic work by Hodgkin and Huxley[1, 2, 3, 4] who have summarized their experimental studies of the giant axon of the squid in four differential equations. In HH model and more generally in conductance based model, membrane ion channels are considered as a conductors and lipid bilayer works as a capacitor. In this model a neuron is represented by a single isopotential electrical compartment, without effective sub cellular ionic movement and only its transmembrane ionic movements was considered. Moreover neural excitability is explained based on membrane capacitance, I_c, and ion channels conductance. Each ion has a selective ion channel and passing of each ion through membrane produces a transmembrane current. Thus, the total membrane current, $I_m(t)$, is the sum of the capacitive current and the ionic currents. For example in HH model $I_m(t) = I_c + I_{ionic}$, where $I_c = C_m \frac{dv(t)}{dt}$

is capacitive current and $I_{ionic} = I_{Na} + I_K + I_L$ is the sum of ionic currents, which I_{Na} and I_K are produced by sodium and potassium ions respectively and I_L denoted to leak current which is an approximation of passive properties of membrane. Conductance (inverse of resistance) and driving force determine ionic current intensity. Thus

$$I_{ionic} = g_{Na}(v)[v(t) - E_{Na}] + g_K(v)[v(t) - E_K] + g_L[v(t) - E_L].$$

The dynamics of a voltage-gated ionic channel is modeled by the conventional Hodgkin-Huxley mathematical description. In that description, the dynamics of the ionic channel activation and inactivation gates are modeled by a first-order differential equation dependent on the gate variables and the membrane potential. For example a current due to ionic species S with an activation gating variable and without inactivation variable, would be given by $g_s = \bar{g}_s \times a$, where a is described by first-order kinetics and $\bar{g}_s$ represents the maximal conductance for the particular ion channel. Therefore, the basic formulation for conductance-based model is as follow:

$$C_m \frac{dv}{dt} = I_{ext} - \sum_j g_j(v - E_j) \tag{1}$$

where $g_j = \bar{g}_j a_j^x b_j^y$ with $\frac{da_j}{dt} = \frac{a_{\infty,j}(v) - a_j}{\tau_{a_j}(v)}$ and $\frac{db_j}{dt} = \frac{b_{\infty,j}(v) - b_j}{\tau_{b_j}(v)}$. In (1) E_j and $(v - E_j)$ are the reversal potential and driving force for j-th ion respectively and I_{ext} is an external current that may be present. Variables of a and b are gating variables and each one has its integer power x and y, respectively. Variables a_∞ and b_∞, are steady state gating variable functions that are typically sigmoidal in shape. The function τ_{b_j} for each j is a time constant which can be voltage-dependent. Thus conductance-based models are consisting of a set of ordinary differential equations based on Kirchoff's laws. The reader is referred to [7] for more details. The Morris-Lecar model is represented by the following three dimensional differential equations:

$$\begin{aligned} C\dot{v} &= i - g_L(v - E_L) - g_{Ca} m_\infty(v)(v - E_{Ca}) - g_K n(v - E_K), \\ \dot{n} &= \phi \frac{n_\infty(v) - n}{\tau_n}, \\ \dot{m} &= \frac{m_\infty(v) - m}{\tau_m} \end{aligned} \tag{2}$$

where

$$\begin{aligned} m_\infty(v) &= \frac{1}{2}\left[1 + \tanh\left(\tfrac{(v - v_1)}{v_2}\right)\right] = \frac{1}{1 + exp(\frac{v_1 - v}{2v_2})}, \\ n_\infty(v) &= \frac{1}{2}\left[1 + \tanh\left(\tfrac{(v - v_3)}{v_4}\right)\right] = \frac{1}{1 + exp(\frac{v_3 - v}{2v_4})}, \\ \tau_n(v) &= 1/\cosh\left(\tfrac{(v - v_3)}{2v_4}\right). \end{aligned}$$

In this model, there exist three kind of ion channels: a potassium, a leak, and a calcium channels. More details about the parameters can be found in [7]. In this paper it is assumed first that $\frac{\phi}{\tau_n(v)} = 1$ and then the results are generalized such that they are applicable on Morris-Lecar model. Moreover the following constraints are assumed on the parameter space:

1. g_L, g_{Ca} and g_K are always positive.
2. E_L, $E_K < 0$ and $E_{Ca} > 0$ so that $E_K < E_L < E_{Ca}$.
3. The applied current, i, is always nonnegative.

3 Mathematical analysis of model.

In this section some preliminary analysis and results for ML model are presented. Using these results the equilibrium points are classified. The ML model (2) can be reduced to the following two dimensional differential equations[7]:

$$\begin{aligned} C\dot{v} &= i - g_L(v - E_L) - g_{Na} m_\infty(v)(v - E_{Na}) - g_K n(v - E_K) \\ \dot{n} &= \phi \frac{[n_\infty(v) - n]}{\tau_n}. \end{aligned} \tag{3}$$

By rescaling time $\theta = Ct$ and replacing ϕ/C by ϕ, it is possible to omit C. Now suppose that $\dfrac{\phi}{\tau_n(v)} = 1$ and consider the following dynamical system:

$$\begin{aligned} \dot{v} &= F_1(v,n) = i - \overbrace{g_L(v - E_L)}^{I_L} - \overbrace{g_{Na} m_\infty(v)(v - E_{Na})}^{I_{Na,p}} - \overbrace{g_K n(v - E_K)}^{I_K} \\ \dot{n} &= F_2(v,n) = n_\infty(v) - n \end{aligned} \tag{4}$$

which is also called ML model. Here $F = (F_1, F_2)$ is a vector field which is clearly analytic. We will show that geometrical properties of two nullclines of (4), that is, $F_1 = 0, F_2 = 0$ together with divergence curve ($\mathrm{div} F = \frac{\partial F_1}{\partial v} + \frac{\partial F_2}{\partial n} = 0$) and $n = I_\infty(v)$, which is defined in (13), are sufficient for the classification of equilibriums of (4). The nullclines of (4) can be written as follows:

$$n := f(v) = \frac{i - g_L\,(v - E_L) - g_{Ca} m_\infty(v)\,(v - E_{Ca})}{g_K\,(v - E_K)} \tag{5}$$

$$n := g(v) = n_\infty(v). \tag{6}$$

Theorem 3.1. *For any values of parameters in biological range, the v-nullclines of (4) is strictly decreasing or it has only one minimum and one maximum point.*

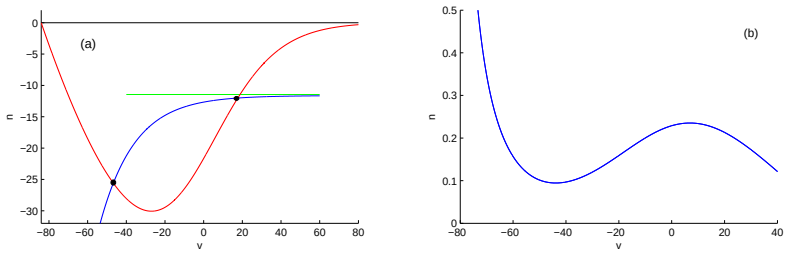

Figure 1: (a):Intersection of these two cures are extremums of $n = f(v)$ plotted in (b).

Proof. The result follows from the first derivative test. Suppose that $E_K < E_L < E_{Ca}$ and $i > 0$. First note that:

$$\lim_{v\to-\infty} f(v) = \frac{-g_L}{g_K},\ \lim_{v\to+\infty} f(v) = \frac{-g_L - g_{Ca}}{g_K},\ \lim_{v\to E_K^{\pm}} f(v) = \pm\infty.$$

Thus, three lines $n = \dfrac{-g_L - g_{Ca}}{g_K}$, $n = \dfrac{-g_L}{g_K}$ and $v = E_K$ are right, left horizontal and vertical asymptotes for $n = f(v)$, respectively. On the other hand, we can write $f'(v)$ as follows:

$$\begin{aligned} f'(v) &= \frac{df(v)}{dv} \\ &= \frac{-i + g_L(E_K - E_L) - g_{Ca}m'_\infty(v)(v - E_{Ca})(v - E_K) - g_{Ca}m_\infty(v)(E_{Ca} - E_K)}{g_K(v - E_K)^2}. \end{aligned}$$

It is easy to check that in the interval $(-\infty, E_K]\cup[E_{Ca}, +\infty)$, $f'(v)$ is negative, so the extremums of $n = f(v)$ lay between $[E_K, E_{Ca}]$ if they exist. If $f'(v) = 0$ then:

$$-i + g_L(E_K - E_L) = g_{Ca}m'_\infty(v)(v - E_{Ca})(v - E_K) + g_{Ca}m_\infty(v)(E_{Ca} - E_K) \tag{7}$$

using $m'_\infty(v) = \frac{1}{v_2}e^{(v_1-v)/v_2}m^2_\infty(v)$, (7) can be rewritten as follow:

$$\frac{g_L(E_K - E_L) - i}{g_{Ca}}(1+e^{(v_1-v)/v_2}) = [\frac{1}{v_2}e^{(v_1-v)/v_2}m_\infty(v)(v - E_{Ca})(v-E_K)+(E_{Ca} - E_K)]. \tag{8}$$

Then the extremums can be obtained by solving the equations:

$$n = \frac{g_L(E_K - E_L) - i}{g_{Ca}}(1 + e^{(v_1-v)/v_2}) - (E_{Ca} - E_K) \tag{9}$$

$$n = \frac{1}{v_2}e^{(v_1-v)/v_2}m_\infty(v)(v - E_{Ca})(v - E_K) \tag{10}$$

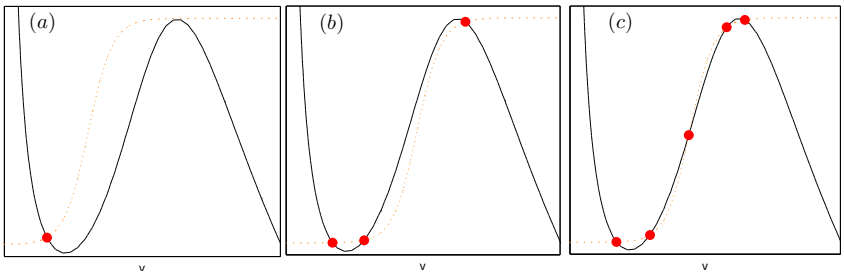

Figure 2: Some examples of different number of equilibrium points in ML model.

The graphs of (9) and (10) are drawn in Fig. 1.a. The shapes of (9) and (10) remain constant for the values of the parameters in their respective ranges. Since these two curves, can intersect each other in at most two points, thus $n = f(v)$ have at most two extremums in (E_K, E_{Ca}). From the continuity and asymptotic behaviour of $n = f(v)$ in (E_K, E_{Ca}), it is easy to see that the left extremum is a minimum and the right one is a maximum point. □

Corollary 3.1. *Suppose that in the range where $n = f(v)$ has positive slope, the equation $f''(v) = 0$ has one solution, then (4) has at most five equilibrium points.*

Proof. The equilibrium of system (4) lies in the intersection of $n = f(v)$ and $n = g(v)$. The result is obtained by applying theorem 3.1 and the fact that $g(v)$ is strictly increasing and $g''(v)$ changes sign only one time. □

Typical graphs of nullclines and their intersections are drawn in Fig. 2.

Definition 3.1. *The curve* $\mathrm{div}F = 0$ *is called divergence curve. It is easy to check that divergence curve is represented as follows:*

$$n = c(v) = \frac{-g_L - g_{Ca}m'_\infty(v)(v - E_{Ca}) - g_{Ca}m_\infty(v) - 1}{g_K}. \tag{11}$$

As it is shown later, the graph of (11) and its intersection with $n = f(v)$ has an important role to determine phase portraits and qualitative behavior of ML model.

Theorem 3.2. *For any parameter value, the divergence curve (11) has exactly one minimum and one maximum points.*

Proof. First note that:

$$\lim_{v\to-\infty} c(v) = -\tfrac{g_L+1}{g_K}, \lim_{v\to+\infty} c(v) = -\tfrac{g_L+g_{Ca}+1}{g_K}.$$

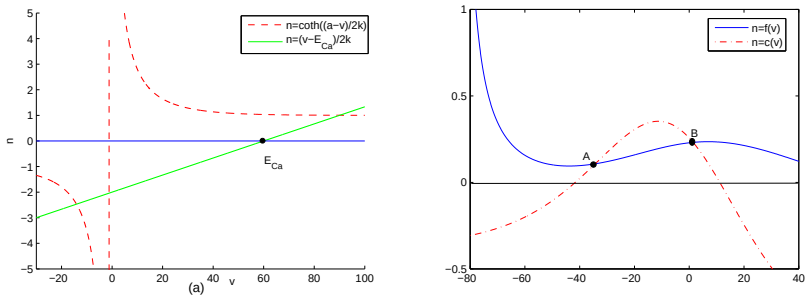

Figure 3: (a):Intersection of these two curves is extremums of $n = c(v)$. (b):Intersection of divergent curve and v nullcline.

Thus $n = -\frac{g_L+1}{g_K}$ and $-\frac{g_L+g_{Ca}+1}{g_K}$ are left and right horizontal asymptotes for $n = c(v)$. On the other hand it is easy to see that

$$\begin{aligned} c'(v) &= \frac{-2g_{Ca}m'_\infty(v) - g_{Ca}m''_\infty(v)(v-E_{Ca})}{g_K} \\ &= -\frac{g_{Ca}m'_\infty(v)}{g_K}[2 + \frac{1}{v_2}m(e^{\frac{v_1-v}{v_2}} - 1)(v-E_{Ca})]. \end{aligned} \tag{12}$$

Thus, the solutions of $c'(v) = 0$ are obtained from the intersections of these two curves:

$$\begin{cases} n = \dfrac{(v-E_{Ca})}{2v_2} \\ n = -\dfrac{1}{m_\infty(v)(e^{\frac{v_1-v}{v_2}} - 1)} = -\dfrac{e^{\frac{v_1-v}{v_2}} + 1}{e^{\frac{v_1-v}{v_2}} - 1} = -\coth\left(\dfrac{v_1-v}{2v_2}\right). \end{cases}$$

The graphs of these two functions are drawn in Fig. 3. In this figure, it is obvious that the roots of (12) are the intersection of a straight line and the "$-\coth$" function which these intersections always occur in two points so that one of them is less than E_{Ca} and the other is larger than E_{Ca}. On the other hand,

$$c''(v) = (\frac{m''_\infty(v)}{m'_\infty(v)} - \frac{1}{v-E_{Ca}})c'(v) + \frac{m'_\infty(v)g_{Ca}}{g_K(v-E_{Ca})}[\frac{2}{(v-E_{Ca})^2} + \frac{1}{2v_2}(1-\tanh^2(\frac{v_1-v}{2v_2}))].$$

So if v^* is a root of (12) with $v^* < E_{Ca}$ then $c''(v^*) < 0$, hence the second derivative test implies that the smaller extremum of $n = c(v)$ is a maximum point and the other is minimum. The graph of $c(v)$ for some values of parameters is shown in Fig. 3.b. □

Remark 3.1. *The roots of $f(v) = 0$ are obtained by intersecting the following curves:*

$$n = \frac{i - g_L(v - E_L)}{g_{Ca}(v - E_{Ca})}$$
$$n = m_\infty(v).$$

If $i < g_L(E_{Ca} - E_L)$ then $f(v) = 0$ has at most three roots in $[E_K, E_{Ca})$ and otherwise it has exactly one root in $[E_{Ca}, +\infty)$. If v^* is the greatest root of $f(v) = 0$, then it is easy to see that the rectangular $D := (E_K, v^*] \times [0, 1]$ is positively invariant under the flow of (4). Since (4) has not any equilibrium point outside of D, and $\dot{n} < 0$ on the line $n = 1$, thus there is no closed orbit outside of D. So in order to qualitative analysis of (4), it is sufficient to consider it in D.

Theorem 3.3. *Two curves $n = f(v)$ and $n = c(v)$ can intersect at most in two points. Moreover these intersections occur in the region where $n = f(v)$ has positive slope.*

Proof. It is easy to see that :

$$g_K(c(v) - f(v)) = g_K(v - E_K)f'(v) - 1$$

so if $f'(v) < 0$ then the above equation do not have any root. □

Definition 3.2. *We call two points of intersections of $n = f(v)$ and $n = c(v)$ in Theorem 3.3 Hopf points and denote them by $A = (v_A, n_A)$ and $B = (v_B, n_B)$.*

Theorem 3.4. *If $n = f(v)$ and $n = c(v)$ does not intersect then the system (4) does not have any limit cycle.*

Proof. By remark 3.1, it is suffice to prove that (4) has not any limit cycle in D. Let $s(v) = \dfrac{1}{v - E_K}$ and consider the following system of differential equations:

$$\dot{v} = s(v)F_1(v, n)$$
$$\dot{n} = s(v)F_2(v, n)$$

Since:

$$\nabla\cdot(s(v)F) = (f(v) - c(v))s(v)$$

so $\nabla\cdot(s(v)F)$ is not identically zero and does not change sign in D by the assumption. Thus the system has not any limit cycle by applying Dulac's criteria. □

Remark 3.2. *Because the proof does not depends on the choice of $\tau_n(v)$, Theorem 3.4 is also valid for arbitrary time constant $\tau_n(v)$.*

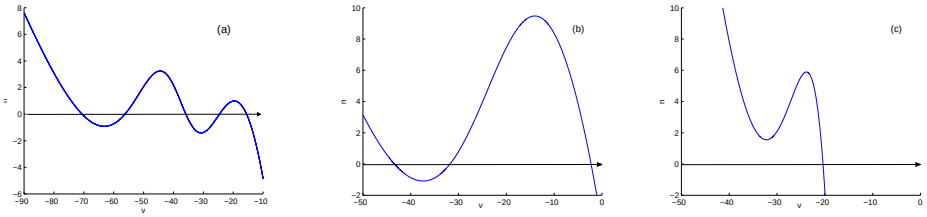

Figure 4: The graph of $n = I_\infty(v)$, corresponding to parameters in Fig. 2 respectively.

Lemma 3.1. *Let* Γ *be a limit cycle for (4). Then* Γ *must contain at least one of two points* A *or* B *in its interior.*

Proof. From Poincaré Index theory, if Γ is a limit cycle of (4) then it must contains at least one equilibrium point in its interior and sum of the indices of equilibrium points in the interior of Γ is equal 1. Moreover by applying Dulack's criteria in theorem 3.4 it is shown that every limit cycle of (4), must be intersected at least one of the two vertical lines $v = v_A$ or $v = v_B$. Thus, it is obvious that any limit cycle Γ of (4), if any, must contain at least one of the two points A or B, on its interior. □

More useful information about the dynamics of (4) can be derived from $n = I_\infty(v)$, which is defined as follow:

$$n = I_\infty(v) = i - g_L(v - E_L) - g_{Ca} m_\infty(v)(v - E_{Ca}) - g_K n_\infty(v)(v - E_K). \quad (13)$$

It is clear that if v_0 is a root of $I_\infty(v) = 0$, then $(v_0, n_\infty(v_0))$ is an equilibrium of (4). On the other hand if $v \to \pm\infty$ then $I_\infty(v) \to \mp\infty$ and thus continuity of it and corollary 3.1 results that it has at most five roots. The graph of (13) is similar to one of the graphs presented in Fig. 4.

Lemma 3.2. *If* (v_0, n_0) *is an equilibrium of (4) Then* $\det(J(v_0, n_0)) = -I'_\infty(v_0)$. *Here* $J(v_0, n_0)$ *is the Jacobian matrix of linearization of (4) at* (v_0, n_0).

Proof. Since $n_0 = n_\infty(v_0)$, the results are obtained from an straightforward calculation. □

Corollary 3.2. *Suppose that* v_0 *is a simple root of* $I_\infty(v) = 0$, *i.e,* $I'_\infty(v_0) \neq 0$. *If* $I'_\infty(v_0) > 0$, *then* $(v_0, n_\infty(v_0))$ *is a saddle equilibrium point of (4).*

Thus if $I_\infty(v)$ have three roots then the middle root always is a saddle equilibrium point for (4). The same result holds for second and fourth root of $I_\infty(v) = 0$ if it has five roots.

Corollary 3.3. *The point* (v_0, n_0) *is a hyperbolic equilibrium of (4) if* v_0 *is a simple root of* $I_\infty(v) = 0$ *and* $v_0 \neq v_A$, $v_0 \neq v_B$.

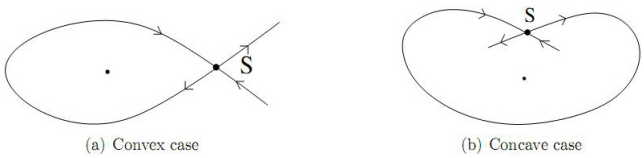

Figure 5: Two cases of homoclinic loops L.

Corollary 3.4. *If $I_\infty(v) = 0$ has either two or four roots then at least one equilibrium of (4) is non hyperbolic.*

Proof. Since

$$\lim_{v\to\pm\infty} I_\infty(v) = \mp\infty$$

the continuity of $I_\infty(v)$ implies that one root must satisfy the equation $I'_\infty(v) = 0$ and by Corollary 3.3, the system (4) has a non hyperbolic equilibrium point. □

Theorem 3.5 (linear stability of hyperbolic equilibriums)**.** *Let $P_i = (v_i, n_i)$, $i = 1, ..., k$, be hyperbolic equilibrium points of (4) such that for $i < j$, $v_i < v_j$, then*

1. *if k=1, then P_i is anti-saddle and if $v_A < v_i < v_B$ then P_i is unstable, otherwise it is stable.*
2. *if k=3, then P_2 is a saddle equilibrium point. For $i = 1, 3$, if $v_A < v_i < v_B$ then P_i is unstable, otherwise it is stable.*
3. *if k=5, then P_2 and P_4 are saddle equilibrium points. For $i = 1, 3, 5$, if $v_A < v_i < v_B$ then P_i is unstable otherwise it is stable.*

Proof. The results follow form Corollary 3.2, Corollary 3.3, and the classification theorem of equilibriums of two dimensional dynamical systems [11]. □

4 On the existence of Homoclinic loop.

In this section some definitions and results related to the existence and stability of homoclinic and double homoclinic loops in ML Model are presented. Consider a planar dynamical system

$$\dot{X} = F(X); \quad X = (x, y) \in R^2 \tag{14}$$

where $F = (f, g) : R^2 \to R^2$ is a C^∞ vector field. A homoclinic orbit is a trajectory of (14) whose ω-limit and α-limit sets are a saddle equilibrium point S of (14). Suppose that the vector field (14) has a homoclinic loop consisting

of a homoclinic orbit L and a hyperbolic saddle point S. For simplicity, L is also called a homoclinic loop. Since the saddle S is hyperbolic, we can define a Poincaré map on one and only one side of a given loop L. More precisely, if we suppose that L is oriented clockwise, then there are two possible cases: convex (Fig. 5.a) and concave (Fig. 5.b). The Poincaré map is well defined near L in the interior of L, $Int(L)$, for the convex loop, and in the exterior of L, $Ext(L)$, for the concave loop. Hence we can define interior (exterior) stability of convex (concave) loop. For the convex case, if there exists a neighbourhood U of L such that for any point $A \in U \cap Int(L)$, $\omega(A) = L$ ($\alpha(A) = L$) then L is said to be out stable (unstable). A similar definition exists for the concave case. It is known that [16, 12] in (14), if $c_1 = (f_x + g_y)(S) < 0$ (resp. > 0), then L is stable (resp. unstable). The saddle is called weak if $c_1 = 0$. Moreover for a homoclinic loop with weak saddle equilibrium of a given planar vector field, a sequence of quantities, is defined to study the stability and bifurcations of the loop. Among these quantities, the first non-zero one determines the stability of the homoclinic loop [8]. A double homoclinic loop consists of a saddle point with two homoclinic orbit. We can define the stability of a double homoclinic like what was defined for homoclinic loop in both exterior and interior side. On the other hand Poincaré- Bendixson theorem implies that if the homoclinic loop with hyperbolic saddle exists then it has at least one equilibrium point in its interior. Moreover for ML model from Theorem 3.5 it is clear that if S is a saddle equilibrium then, c_1, the saddle quantity of S, is positive if $v_A < v_S < v_B$ and negative if $v_S < v_A$ or $v_B < v_S$. The saddle is weak if $S \in \{A, B\}$. Since S is hyperbolic, the homoclinic loop contains at least one equilibrium point of (4) in its interior. The following result provides some conditions for the existence of homoclinic loop and determines its stability in ML model.

Theorem 4.1. *Each homoclinic loop L of (4) with non positive saddle quantity must contain either A or B in its interior.*

Proof. Let $S = (v_s, n_s)$ be a saddle equilibrium of (4) with negative quantity. Without loss of generality suppose $v_s < v_A$. If L does not contain A and B in its interior then, the equilibrium point P, which is in the interior of L, is stable. On the other hand since L and P are both stable then there exists at least one limit cycle Γ in the interior of L as a separator of basin of attraction of P and L, we derive a contradiction with Lemma 3.1. □

Corollary 4.1. *Suppose that the saddle quantity of (4) is negative. Then it cannot have any double homoclinic loop.*

5 Classification of phase portraits.

In this section, by applying the results that obtained in sections 3, 4 together with some classical theorems of planar dynamical systems, in the case that all

three equilibrium points of (4) are hyperbolic, all possible phase portraits of ML model are classified. Note that we restrict ourselves to all physiological constraints on parameter space which was mentioned in section 2. By remark 3.1, it is sufficient to consider the phase portrait in rectangular $D = (E_K, v^*] \times [0, 1]$ where v^* is the greatest root of $f(v) = 0$. All trajectories which start from the exterior of D come into the interior of D after a certain time, i.e., D is a positively invariant set.

Definition 5.1. *A segment for (4) is a maximal invariant, compact and connected subset containing an anti-saddle equilibrium and no other equilibrium point of (4).*

Definition 5.2. *Two phase portraits X and Y for (4) are said to be conjugate* ***up to segments*** *if by collapsing every segment at some point, the produced phase portraits can be conjugated.*

The segment may consist of a single equilibrium point, otherwise its boundary is necessarily a limit cycle of system (4). Segments which consist of a single equilibrium point are named segment of type 1, and the others are named of type 2. As a Jordan curve, a segment of type 2 probably has many limit cycles in its interior. But since (4) is an analytic dynamical system, according to Poincaré's theorem [11], the number of these limit cycles are finite. The stability of a segment is defined as the stability of invariant set. Fig. 7 shows some examples of different kind of possible segments for system (4), which are drawn with Matlab software. If two curve $n = c(v)$ and $n = f(v)$ does not intersect each other, i.e., two points A and B do not exist, then Theorems 3.4 and 3.5 imply that all segments must be stable equilibriums. In this case, according to the number of equilibriums, the phase portrait of ML model is conjugated with one of the phase portraits shown in Fig. 6. In the rest of this section we assume that there exists two different Hopf points.

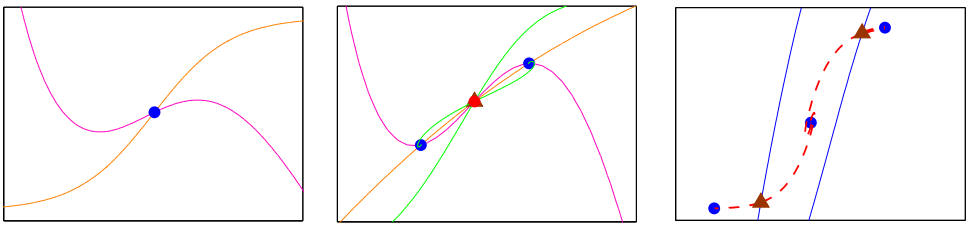

Figure 6: In the absence of A and B, there exist no closed orbit.

5.1 Phase portraits with one segment.

In the case that (4) has only one equilibrium point, it is clear that this point is an anti-saddle. Thus the phase portrait of (4) has only one segment. Since

the rectangular D is positively invariant, this segment is necessarily stable. So if $P = (v_p, n_p)$ is an unstable equilibrium, i.e., v_p, satisfies $v_A < v_p < v_B$, then the segment is necessarily of type 2. In this case, if there is exactly one limit cycle that contains a stable equilibrium, then the cycle is necessarily saddle cycle and therefore the system is structurally unstable. Some examples of this case are illustrated in Fig. 7.

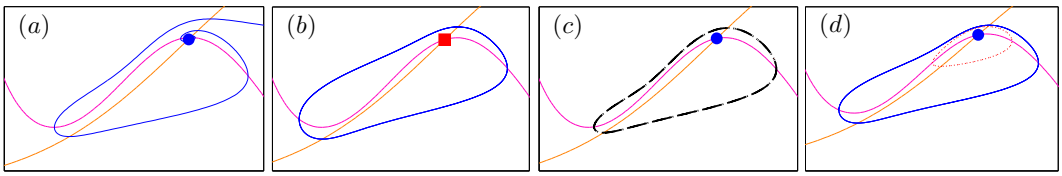

Figure 7: Possible phase portraits of ML model with one segment.

5.2 Phase portraits with two segments.

In the case, that (4) has more than one equilibrium point, hyperbolicity of equilibriums and Corollary 3.3 imply that there are at least three equilibrium points and one of them is saddle. If the system (4) has three equilibrium points then there exist probably some limit cycles, which contain all equilibrium points. For example in the case that all segments are unstable, positive invariantness of D, the Poincaré-Bendixson theorem and the Poincaré index theory [11], guarantees the existence of such a limit cycle.

Definition 5.3. *A separator cycle is a limit cycle of (4) whit minimal topological diameter that as a Jordan curve, contains all equilibrium points of (4) in its interior.*

Suppose that (4) has three equilibrium points. Let W^s and W^u denote stable and unstable manifolds of saddle point S respectively. Then $W^s = W_1^s \cup W_2^s \cup \{S\}$ and $W^u = W_1^u \cup W_2^u \cup \{S\}$ where W_i^s and W_i^u, for $i = 1, 2$ are two branches of W^s and W^u respectively.

Class A: There is no separator cycle. The existence of W^u and positive invariantness of rectangular D imply that at least one segment must be stable. The other segment may be stable or unstable.

A-1 Homoclinic loop does not exist. Due to the existence of W^u, one segment must be necessarily stable. The other segment can be either stable or unstable. If it is unstable then the stable segment must attracts both W_1^u and W_2^u which produces an invariant set with $\overline{W^u}$ as its boundary. This implies that the unstable segment is contained in this invariant set. The fact that W^s and W^u transversally intersect implies

that either W_1^s or W_2^s originates from infinity and the other one must be repelled by an unstable segment.(see Fig. 8.a). If two segments are stable then the phase portrait is as Fig. 8.b.

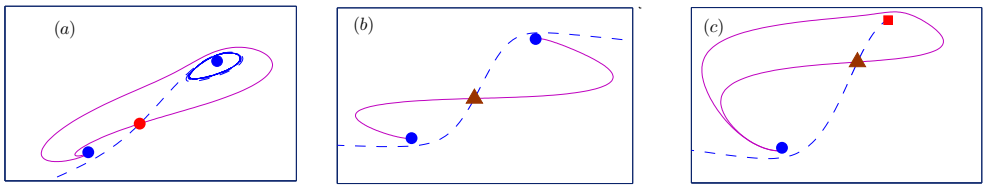

Figure 8: Some possible phase portraits for ML model with no separator cycle and no saddle loop up to segments.

A-2 There exists a homoclinic loop. Suppose there exists a homoclinic loop L. As before one segment must be stable. In the convex case, the inner stability of L is the opposite stability of the segment which is contained in its interior. The outer segment is necessarily an stable segment and it is an ω-limit set of one branch of W^u. Other branch of W^s arises from infinity. If homoclinic is concave, then it must be outer stable, hence the saddle quantity must be non-positive, i.e., $c_1 \leq 0$. Without loss of generality, suppose $v_S < v_A$ where v_S is the potential of saddle point S. Then Theorem 4.1 implies that the left segment is necessarily a stable equilibrium which attracts one branch of W^u. The other segment must be unstable because S is hyperbolic saddle and the result is obtained from the Poincaré-Bendixson theorem. Phase portraits of ML model in this case is shown in Fig. 9.

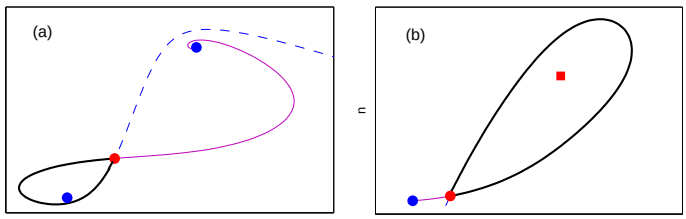

Figure 9: Some examples of case A-2 up to segments. (a)$c_1 > 0$ (b) $c_1 < 0$.

A-3 There exists a double homoclinic loop H**.** For the convex case, outer stability of H implies $c_1 \leq 0$. On the other hand, Corollary 4.1 implies that $c_1 \geq 0$, thus $c_1 = 0$. This means that saddle point is weak, i.e., it is either A or B. Corollary 4.1 implies that one of the segments is necessarily an stable equilibrium and its surrounding loop is unstable from inside and stable from outside.

Class B:There is an inner stable separator cycle Γ. We recall that, the existence of a separator cycle Γ, which contains all equilibrium points, is possible in the phase portrait of ML model. For example in the case that all segments are unstable, the existence of such cycle is guaranteed by the positively invariant property of the rectangular D.

B-1 There is no homoclinic loop. Due to the existence of W^s, one segment must be necessarily unstable. The other segment can be either stable or unstable.
If it is stable then the unstable segment must repel both W_1^s and W_2^s which produces an invariant set with W^s as its boundary. This implies that the stable segment is contained in this invariant set. The fact that W^s and W^u transversally intersect implies that one of W_1^u or W_2^u is attracted by the separator cycle Γ and the other one must be attracted by an stable segment (see Fig. 10.a). If two segments are unstable the phase portrait is as in Fig. 10.b.

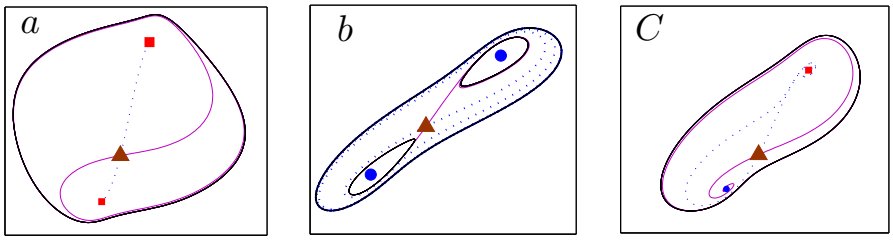

Figure 10: Some examples of case B-1 up to segments.

B-2 There is a homoclinic loop L. First suppose that L is convex. Because the saddle point is hyperbolic and Γ is inner stable, the segment which is outside of L must be unstable. If L is concave then it must be outer unstable since Γ is inner stable. Thus the saddle quantity in this case must be non negative. Then, one of the segments must be stable and the other one must be unstable. See Fig. 11.

B-3 There is a double homoclinic loop H. Suppose H is convex. Since Γ is inner stable so H must be outer unstable and thus $c_1 \geq 0$. In other words $v_A < v_S < v_B$. This implies that two segments must be stable if the saddle is not weak. Otherwise according to Corollary 4.1 one of the loops of H contains one stable segment of type 1, i.e., an stable equilibrium which implies that this loop is both inner and outer unstable. If H is concave, then it is outer unstable, since Γ is inner stable. Thus $c_1 \geq 0$. If $c_1 \neq 0$ the Poincaré-Bendixson and inner stability of Γ implies that both segments must be stable.

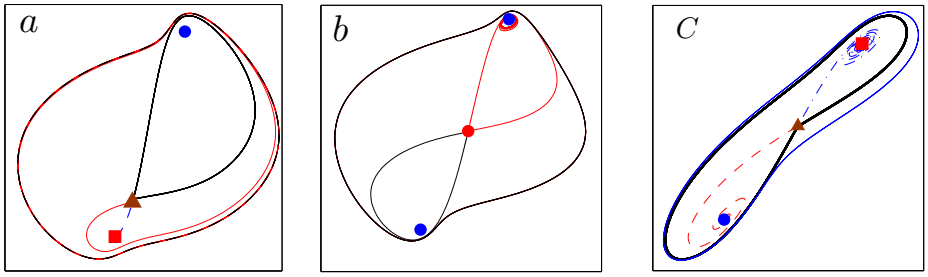

Figure 11: Some examples of case B-2 up to segments.

Class C: There is an inner unstable separator cycle Γ.

C-1 There is no homoclinic loop. Due to the existence of W^u, one segment must be necessarily stable. The other segment can be either stable or unstable.
If it is unstable then the stable segment must attract both W_1^u and W_2^u which produces an invariant set with W^u as its boundary. This implies the unstable segment is contained in this invariant set. The face that W^s and W^u transversally intersect implies that one of the sets W_1^s or W_2^s is repelled by the separator cycle Γ and the other one must be repelled by unstable segment.

C-2 There is a homoclinic loop L. First suppose that L is convex. Because saddle point is hyperbolic and Γ is inner unstable, the segment which is outside of L must be stable. If L is concave then it must be outer stable since Γ is inner unstable. Thus the saddle quantity in this case must be non positive. Then one segment must be stable and the other one must be unstable.

C-3 There is double homoclinic loop H. Suppose H is convex. Since Γ is inner unstable so H is outer stable and $c_1 \leq 0$. On the other hand Corollary 4.1 implies that $c_1 \geq 0$, thus $c_1 = 0$. This means that saddle point is weak, i.e., it is either A or B. Corollary 4.1 implies that one of the segments is necessarily an stable equilibrium and its surrounding loop is unstable from inside and stable from outside.

6 Extended results.

Up to now we have supposed that $\tau_n(v) = 1$ (and $i > 0$), but in ML model we have $\frac{1}{\tau_n(v)} = cosh\frac{v-v_3}{2v_4}$, and the last function is positive and strictly convex function. The goal of this section is to show that the previous results are valid for every choice of $\tau_n(v)$ where $\frac{1}{\tau_n(v)}$ is positive and convex. In particular the

results are true for ML model. To see this, consider the dynamical system

$$\begin{aligned} \dot{v} &= i - g_L(v - E_L) - g_{Na} m_\infty(v)(v - E_{Na}) - g_K n(v - E_K) \\ \dot{n} &= \frac{[n_\infty(v) - n]}{\tau_n}. \end{aligned} \tag{15}$$

Now suppose that $\frac{1}{\tau_n(v)}$ is positive and strictly convex function and all parameters are as before. Two dynamical system (4) and (3) have the same nullclines, thus they have the same number of equilibriums. In addition every saddle point $P_0 = (v_0, n_0)$ of (4) is also a saddle of (3) and vice-versa. Note that curve defined in (13) is the same for the dynamical systems (4) and (3). On the other hand if $\bar{J}$ is the Jacobian of linearization of (3) at P_0 then

$$\det(\bar{J}) = -\frac{1}{\tau_n(v)} I'_\infty(v_0).$$

Then saddle is related to saddle and vice versa. The divergence curve of (3) is as follow:

$$n = \bar{c}(v) = \frac{-g_L - g_{Ca} m'_\infty(v)(v - E_{Ca}) - g_{Ca} m_\infty(v) - \frac{1}{\tau_n(v)}}{g_K} \tag{16}$$

and by (11) it follows that

$$g_K \bar{c} = g_K c(v) - \frac{1}{\tau_n(v)} + 1 \tag{17}$$

where $n = c(v)$ is the divergence curve of (4). One may wonder that additional term $-\frac{1}{\tau_n(v)} + 1$ in the right hand side of (17) changes the number and relative position of Hopf points (Definition 3.2) for (15). The following results states that this does not happen if $\frac{1}{\tau_n(v)}$ is positive and strictly convex function.

Theorem 6.1. *If $\frac{1}{\tau_n(v)}$ is positive and strictly convex function then divergence curve and v- nullcline of (15) have at most two intersection points. these intersections occur in the region where v-nullcline has positive slope.*

Proof. The following equation is satisfied for (15)

$$g_k(v - E_k) f'(v) = g_k(\bar{c}(v) - f(v) + \frac{1}{\tau_n(v)} \tag{18}$$

thus the intersection points of $n = \bar{c}(v)$ and $n = f(v)$ are obeyed the equation

$$g_k(v - E_k) f'(v) = \frac{1}{\tau_n(v)} \tag{19}$$

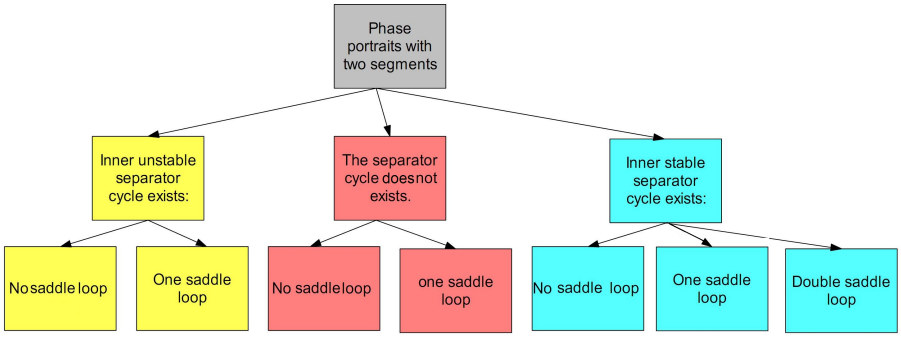

Figure 12: ML model with two segments.

and vice versa. Therefore it is clear that if $f'(v) < 0$ then (19) does not have any solution. On the other hand we suppose that $f''(v) = 0$ has unique root v with $f'(v) > 0$. By Theorem 3.1 it has at most two extremums. Let v_{min} and v_{max} be the roots of $f'(v) = 0$. So by positivity and convexity of $\frac{1}{\tau_n(v)}$, (15) has at most two Hopf points. □

Theorem 6.2. *Let A' and B' be Hopf points of (15) then all statements of Theorem 3.5 are satisfied for (15).*

Theorem 6.3. *If $n = f(v)$ and $n = \bar{c}(v)$ do not intersect then the system (15) do not have any limit cycle.*

Theorem 6.4. *If a phase portrait is not possible for (4) then it is not possible for (15) and vice versa.*

Proof of theorems 6.2, 6.3 and 6.4: These theorems can be proved in the same manner of previous sections.

7 Concluding Remarks

Calculations similar to the previous section show that ML model has at most five equilibrium points. They are contained in the positively invariant rectangular D. Complement of D has a simple dynamics because it contained no invariant set. There exist at most two Hopf points such that every closed orbit must contain at least one of them. In the absence of Hopf points there exist exactly three phase portraits. All interesting phase portraits occur in the presence of Hopf points. It is shown that there are at most 11 non conjugated phase portraits in ML up to segments. The graph of possible phase portraits is sketched in Fig. 12 and Fig. 13. The classification of phase portraits with

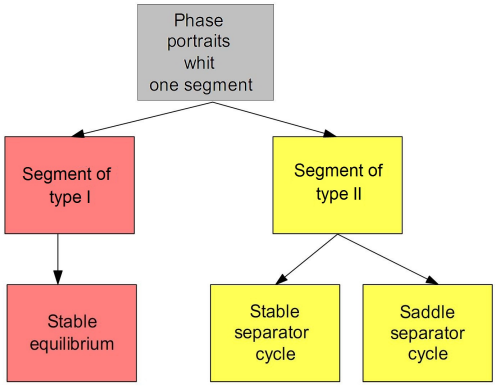

Figure 13: ML model with one segment.

five hyperbolic equilibriums can be obtained in the same manner as previous sections. Finally it is shown that in the case that equilibriums are hyperbolic, ML model and $I_{Na,p} + I_K$ have the same possible phase portraits and this argument is valid for every choice of time constant function $\tau_n(v)$.

figure	i	g_L	E_L	g_{Ca}	E_{Ca}	V_1	V_2	g_k	E_k	ϕ	V_3	V_4
6-a	3	1	-3	7	80	-3	20	-4	-90	1	-30	7
6-b	3	1	-3	7	80	-3	20	-4	-90	1	-110	60
6-c	8	7	-79	21	60	-27	11	-10	-90	30	-39	5
2 -a	8	7	-79	21	60	-27	11	10	-90	1	-15	5
2 -b	8	7	-79	21	60	-27	11	10	-90	1	-9.5	5
2 -c	8	7	-79	21	60	-27	11	10	-90	30	-39	5
7-a	0.2	3.25	-42	7	49.5	-10	10	-4.25	-58.2	1	-15	8
7-b	0.2	3.25	-42	7	49.5	-10	10	-4.25	-58.2	1	-10	8
7-c	0.2	3.25	-42	7	49.5	-10	10	-4.25	-58.2	1	-9.3727011	8
7-d	0.2	3.25	-42	7	49.5	-10	10	-4.25	-58.2	1	-9.5	8
11 a	21	1	-26	3	75	-31	2	12	78	2	-25	6
11 b	1	2	-5	4	54	-3	3	4	-56	1	-2	6.1
11c	9	1	-26	3	75	-30	5	5.9988	-78	5.03	-32.6	8

Table 1: Some parameters corresponding to related figures.

References

[1] A. Hodgkin and A. Huxley, Currents carried by sodium and potassium ions through the membrane of the giant axon of Loligo,*J. Physiol. (London)* **116**(1952a), 449-472.

[2] A. Hodgkin and A. Huxley, The components of membrane conductance in the giant axon of Loligo,*J. Phsyiol. (London)***116** (1952b), 473-496.

[3] A. Hodgkin and A. Huxley, The dual effect of membrane potential on sodium conductance in the giant axon of Loligo,*J. Physiol. (London)***116** (1952c), 497-506.

[4] A. Hodgkin and A. Huxley, A quantitative description of membrane current and its application to conduction and excitation in nerve,*J. Physiol. (London)***117** (1952d), 500-544.

[5] C. Morris and H. Lecar, Voltage Oscillations in the Barnacle Giant Muscle Fiber, *Biophysical Journal* **35** (1981), 193-213.

[6] E. M. Izhikevich, Neural Excitability, Spiking, and Bursting.*International Journal of Bifurcation and Chaos.***10**(2000), 1171-1266.

[7] E. M. Izhikevich,*Dynamical Systems in Neuroscience: The Geometry of Excitability and Bursting,* The MIT Press, Cambridge, MA, 2007.

[8] Han Maoan and Wu Yuhai, The Stability of Double Homoclinic Loops, *Applied Mathematics Letters* **17** (2004), 1291-1298.

[9] J. Keener and J. Sneyd *Mathematical Physiology,* Springer-Verlag, New York, 1998.

[10] J. Nagumo, S. Arimoto, and S. Yoshizawa, An active pulse transmission line simulating nerve axon, *Proc IRE.***50** (1962) 2061-2070.

[11] L. Perko *Differential Equations and Dynamical Systems,* New York: Springer-Verlag, 1996.

[12] M. Han, S. Hu and X. Liu, On the stability of double homoclinie and heteroclinic cycles, *Nonlinear Analysis* **53** (2003), 701-713.

[13] R. FitzHugh, Mathematical models of threshold phenomena in the nerve membrane. *Bull. Math. Biophysics,***17**(1955), 257-278.

[14] R. FitzHugh, Impulses and physiological states in theoretical models of nerve membrane. *Biophysical J.* **1** (1961), 445-466.

[15] R. FitzHugh *Mathematical models of excitation and propagation in nerve,* McGraw-Hill Book Co., N.Y. 1969.

[16] S.N. Chow and J.K. Hale, *Methods of Bifurcation Theory,* Springer, New York, (1982).

Received: January, 2012